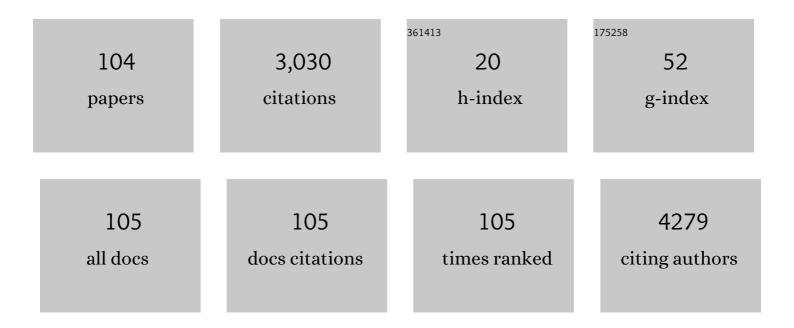
List of Publications by Year in descending order

Source: https://exaly.com/author-pdf/752914/publications.pdf Version: 2024-02-01



DETD LIDICER

#	Article	IF	CITATIONS
1	Influence of structural properties on (de-)intercalation of ClO4â^' anion in graphite from concentrated aqueous electrolyte. Carbon, 2022, 186, 612-623.	10.3	10
2	Chaotropic anion based "water-in-salt―electrolyte realizes a high voltage Zn–graphite dual-ion battery. Journal of Materials Chemistry A, 2022, 10, 2064-2074.	10.3	28
3	Electric and magnetic dipole emission of Eu3+: Effect of proximity to a thin aluminum film. Journal of Luminescence, 2022, 246, 118778.	3.1	5
4	Long-term changes in Al thin-film extreme ultraviolet filters. Applied Optics, 2021, 60, 8766.	1.8	1
5	Optical characterization of low temperature amorphous MoOx, WOX, and VOx prepared by pulsed laser deposition. Thin Solid Films, 2020, 693, 137690.	1.8	11
6	Hard Xâ€ray photoelectron spectroscopy study of core level shifts at buried GaP/Si(001) interfaces. Surface and Interface Analysis, 2020, 52, 933-938.	1.8	8
7	Nanostructure fabrication on the top of laser-made micropillars for enhancement of water repellence of aluminium alloy. Materials Letters, 2019, 256, 126601.	2.6	19
8	Surface Study of Fe3O4 Nanoparticles Functionalized With Biocompatible Adsorbed Molecules. Frontiers in Chemistry, 2019, 7, 642.	3.6	144
9	Non-destructive depth profile reconstruction of single-layer graphene using angle-resolved X-ray photoelectron spectroscopy. Applied Surface Science, 2019, 491, 16-23.	6.1	7
10	Passivation of semipolar (10-1-1) GaN with different organic adsorbates. Materials Letters, 2019, 236, 201-204.	2.6	10
11	Amorphous carbon nanocomposite films doped by titanium: Surface and sub-surface composition and bonding. Diamond and Related Materials, 2018, 81, 61-69.	3.9	16
12	Surface and in-depth distribution of sp2 and sp3 coordinated carbon atoms in diamond-like carbon films modified by argon ion beam bombardment during growth. Carbon, 2018, 134, 71-79.	10.3	39
13	Study of Ni-Catalyzed Graphitization Process of Diamond by <i>in Situ</i> X-ray Photoelectron Spectroscopy. Journal of Physical Chemistry C, 2018, 122, 6629-6636.	3.1	22
14	Spin Seebeck effect in <i>É></i> -Fe2O3 thin films with high coercive field. Journal of Applied Physics, 2018, 124, .	2.5	12
15	Chemical depth profile of layered a-CSiO:H nanocomposites. Applied Surface Science, 2018, 456, 941-950.	6.1	8
16	C sp2/sp3 hybridisations in carbon nanomaterials – XPS and (X)AES study. Applied Surface Science, 2018, 452, 223-231.	6.1	316
17	Effect of treatment at high temperatures on morphology of a carbon supported Pd catalyst investigated by X-ray diffraction and photoelectron spectroscopy aided with QUASES. Applied Surface Science, 2018, 458, 855-863.	6.1	8
18	Electron affinity of undoped and boron-doped polycrystalline diamond films. Diamond and Related Materials, 2018, 87, 208-214.	3.9	14

#	Article	IF	CITATIONS
19	Chemical and structural properties of Pd nanoparticle-decorated graphene—Electron spectroscopic methods and QUASES. Applied Surface Science, 2017, 404, 300-309.	6.1	13
20	Lead-silicate glass surface sputtered by an argon cluster ion beam investigated by XPS. Journal of Non-Crystalline Solids, 2017, 469, 1-6.	3.1	15
21	Pd-catalysts for DFAFC prepared by magnetron sputtering. Applied Surface Science, 2017, 419, 838-846.	6.1	14
22	Influence of the preparation conditions of <scp>Pdâ€ZrO</scp> ₂ and <scp>AuPdâ€ZrO</scp> ₂ nanoparticle–decorated functionalised <scp>MWCNT</scp> s: Electron spectroscopy study aided with the <scp>QUASES</scp> . Surface and Interface Analysis, 2017, 49, 1124-1134.	1.8	4
23	Electron band bending and surface sensitivity: X-ray photoelectron spectroscopy of polar GaN surfaces. Surface Science, 2017, 664, 241-245.	1.9	6
24	Electron band bending of polar, semipolar and non-polar GaN surfaces. Journal of Applied Physics, 2016, 119, .	2.5	21
25	GaN quantum dot polarity determination by X-ray photoelectron diffraction. Applied Surface Science, 2016, 389, 1156-1160.	6.1	4
26	Effect of the Pd/MWCNTs anode catalysts preparation methods on their morphology and activity in a direct formic acid fuel cell. Applied Surface Science, 2016, 387, 929-937.	6.1	39
27	Irradiation of potassiumâ€silicate glass surfaces: XPS and REELS study. Surface and Interface Analysis, 2016, 48, 543-546.	1.8	2
28	Diamond-like carbon and nanocrystalline diamond film surfaces sputtered by argon cluster ion beams. Diamond and Related Materials, 2016, 68, 37-41.	3.9	14
29	Polarity of GaN with polar {0001} and semipolar , , orientations by x-ray photoelectron diffraction. Journal of Materials Research, 2015, 30, 2881-2892.	2.6	8
30	Attenuated total reflectance Fourier-transform infrared spectroscopic investigation of silicon heterojunction solar cells. Review of Scientific Instruments, 2015, 86, 073108.	1.3	12
31	Non-destructive assessment of the polarity of GaN nanowire ensembles using low-energy electron diffraction. Applied Physics Letters, 2015, 106, .	3.3	23
32	In-out asymmetry of surface excitations in reflection-electron-energy-loss spectra of polycrystalline Al. Physical Review B, 2014, 89, .	3.2	6
33	Polarity of semipolar wurtzite crystals: X-ray photoelectron diffraction from GaN{101Â ⁻ 1} and GaN{202Â ⁻ 1} surfaces. Journal of Applied Physics, 2014, 116, .	2.5	6
34	Graphene oxide and reduced graphene oxide studied by the XRD, TEM and electron spectroscopy methods. Journal of Electron Spectroscopy and Related Phenomena, 2014, 195, 145-154.	1.7	1,297
35	Electron Supersurface Scattering On Polycrystalline Au. Physical Review Letters, 2013, 110, 086110.	7.8	19
36	GaN polarity determination by photoelectron diffraction. Applied Physics Letters, 2013, 103, .	3.3	11

#	Article	IF	CITATIONS
37	Atomic and electronic structure of N-terminated GaN(0001̄) (1 × 1) surface. Journal of Physics: Conference Series, 2012, 398, 012013.	0.4	4
38	Hydrogen on nanocrystalline diamond film surfaces. Diamond and Related Materials, 2012, 26, 66-70. Quantitative low-energy electron diffraction analysis of the Gan complimate	3.9	3
39	xmins:mmi="http://www.w3.org/1998/Math/Math/Math/MathIME" altimg="si9.glf" overflow="scroll"> <mml:mrow><mml:mo stretchy="true">(<mml:mn>000</mml:mn><mml:mover) 0.784314="" 1="" 10="" 5<="" etqq1="" overlock="" rgbt="" td="" tf="" tj=""><td>501.6957 To</td><td>d (accent="a</td></mml:mover)></mml:mo </mml:mrow>	501.6957 To	d (ac cent="a
40	Time dependent thermal treatment of oxidized MWCNTs studied by the electron and mass spectroscopy methods. Applied Surface Science, 2012, 258, 7912-7917.	6.1	22
41	Layer-resolved photoelectron diffraction: Electron attenuation anisotropy in GaAs. Journal of Electron Spectroscopy and Related Phenomena, 2012, 185, 184-187.	1.7	1
42	Potassium-silicate glass exposed to low energy H+ beam. Nuclear Instruments & Methods in Physics Research B, 2012, 280, 111-116.	1.4	4
43	Mn incorporation into the GaAs lattice investigated by hard x-ray photoelectron spectroscopy and diffraction. Physical Review B, 2011, 83, .	3.2	12
44	Dielectric response functions of the (0001Â ⁻), (101Â ⁻ 3) GaN single crystalline and disordered surfaces studied by reflection electron energy loss spectroscopy. Journal of Applied Physics, 2011, 110, 043507.	2.5	14
45	Pd/MWCNTs catalytic activity in the formic acid electrooxidation dependent on catalyst surface treatment. Physica Status Solidi (B): Basic Research, 2011, 248, 2516-2519.	1.5	15
46	Influence of Pdâ€Au/MWCNTs surface treatment on catalytic activity in the formic acid electrooxidation. Physica Status Solidi C: Current Topics in Solid State Physics, 2011, 8, 3195-3199.	0.8	11
47	Studies of EPES REELS spectra of polyethylenes aided by line shape analysis—Effect of electron irradiation. Journal of Electron Spectroscopy and Related Phenomena, 2011, 184, 360-365.	1.7	6
48	Reflection electron energy loss spectroscopy of aluminum. Surface Science, 2010, 604, 1006-1009.	1.9	4
49	Comment on: "As 3d core level studies of (GaMn)As annealed under As capping―by I. Ulfat, J. Adell, J. Sadowski, L. Ilver, J. Kanski, Surface Sci. 604 (2010), 125 Surface Science, 2010, 604, 2064.	1.9	0
50	The line shape analysis of electron spectroscopy spectra by the artificial intelligence methods for identification of C sp ² /sp ³ bonds. Physica Status Solidi (B): Basic Research, 2010, 247, 2838-2842.	1.5	8
51	Distinguishing elastic and inelastic scattering effects in reflection electron energy loss spectroscopy. Physical Review B, 2010, 82, .	3.2	3
52	Studies of oxidized carbon nanotubes in temperature range RT–630°C by the infrared and electron spectroscopies. Journal of Alloys and Compounds, 2010, 505, 379-384.	5.5	23
53	Temperature modification of oxidized multiwall carbon nanotubes studied by electron spectroscopy methods. Physica Status Solidi (B): Basic Research, 2009, 246, 2645-2649.	1.5	22
54	Photoemission from α and β phases of the GaAs(001)-c(4×4) surface. Surface Science, 2009, 603, 3088-3093.	1.9	9

#	Article	IF	CITATIONS
55	XPS and XAES of polyethylenes aided by line shape analysis: The effect of electron irradiation. Polymer Degradation and Stability, 2009, 94, 1714-1721.	5.8	13
56	Determination of electron inelastic mean free paths for poly[methyl(phenyl)silylene] films. Polymer, 2009, 50, 2445-2450.	3.8	3
57	Photoemission from Al(100) and (111): Experiment and <i>ab initio</i> theory. Physical Review B, 2008, 78,	3.2	32
58	Effect of electron irradiation on Na–K silicate glass investigated using X-ray photoelectron spectroscopy and pattern recognition method. Journal of Non-Crystalline Solids, 2008, 354, 3840-3848.	3.1	4
59	Photoemission from Al(100): experiment and one-step theory. Journal of Physics: Conference Series, 2008, 100, 072035.	0.4	1
60	Investigation of CoPd alloys by XPS and EPES using the pattern recognition method. Journal of Alloys and Compounds, 2007, 428, 190-196.	5.5	5
61	Role of final states in photoemission from Al(111). Surface Science, 2007, 601, 4105-4108.	1.9	2
62	Attenuation of photoelectrons and Auger electrons leaving nickel deposited on a gold surface. Surface and Interface Analysis, 2007, 39, 916-921.	1.8	6
63	Angular-resolved elastic peak electron spectroscopy: experiment and Monte Carlo calculations. Surface and Interface Analysis, 2006, 38, 615-619.	1.8	15
64	Measurement of the differential electron surface and volume excitation probability in Cu, CuO and Cu2O. Surface and Interface Analysis, 2006, 38, 628-631.	1.8	1
65	Studies of AuNi alloys by electron spectroscopies with the aid of the line shape analysis by the pattern recognition method. Surface and Interface Analysis, 2006, 38, 1204-1210.	1.8	2
66	Determination of the inelastic mean free paths (IMFPs) in Ti by elastic peak electron spectroscopy (EPES): Effect of impurities and surface excitations. Applied Surface Science, 2006, 252, 2741-2746.	6.1	6
67	Valence band photoemission from in-situ grown GaAs(100)-c(4 × 4). European Physical Journal D, 2006, 56, 21-26.	0.4	3
68	UV degradability of polysilanes for nanoresists examined by electron spectroscopies and photoluminescence. European Physical Journal D, 2006, 56, 41-50.	0.4	5
69	Electron surface states in short-period superlattices: (GaAs)2/(AlAs)2(100)-c(4×4). Surface Science, 2006, 600, 3646-3649.	1.9	1
70	The backscattering factor for the Au N67VV Auger transition. Applied Surface Science, 2005, 252, 905-915.	6.1	6
71	Determination of the electron inelastic mean free path for samarium. Surface Science, 2005, 595, 1-5.	1.9	3
72	Studies of iron and iron oxide layers by electron spectroscopes. Applied Surface Science, 2005, 252, 330-338.	6.1	10

#	Article	IF	CITATIONS
73	Electron irradiated potassium-silicate glass surfaces investigated by XPS. Journal of Non-Crystalline Solids, 2005, 351, 1665-1674.	3.1	33
74	Elastic electron backscattering from silicon surfaces: effect of charge-carrier concentration. Surface and Interface Analysis, 2004, 36, 809-811.	1.8	1
75	Elastic electron backscattering from Ti: grain size effect. Surface and Interface Analysis, 2004, 36, 816-819.	1.8	4
76	LEED structural analysis of GaAs(001)-c(4×4) surface. Surface Science, 2004, 566-568, 89-93.	1.9	13
77	Surface excitations in electron backscattering from silicon surfaces. Surface Science, 2004, 562, 92-100.	1.9	31
78	Electron mean free path for GaAs(100)-c(4×4) at very low energies. Surface Science, 2004, 566-568, 1196-1199.	1.9	2
79	Photoelectron escape from iron oxide. Surface Science, 2004, 572, 93-102.	1.9	3
80	Elastic electron backscattering from surfaces in selected angular ranges. Applied Surface Science, 2004, 229, 67-80.	6.1	1
81	GaAs (100)-(1X1) Structure Analysis from LEED Intensities. European Physical Journal D, 2003, 53, 49-54.	0.4	5
82	Scattering angle dependence of the surface excitation probability in reflection electron energy loss spectra. Physical Review B, 2003, 67, .	3.2	43
83	Surface excitation effects in elastic peak electron spectroscopy. Surface Science, 2003, 531, L335-L339.	1.9	24
84	XPS and He II photoelectron yield study of the activation process in Ti–Zr NEG films. Vacuum, 2003, 71, 329-333.	3.5	12
85	Stability of the inelastic mean free paths determined by elastic peak electron spectroscopy in nickel and silicon. Journal of Vacuum Science and Technology A: Vacuum, Surfaces and Films, 2002, 20, 447-455.	2.1	12
86	Growth mode of ultrathin gold films deposited on nickel. Applied Surface Science, 2002, 199, 138-146.	6.1	14
87	Influence of surface composition and density on electron inelastic mean free paths in Ge. Surface and Interface Analysis, 2002, 33, 381-393.	1.8	4
88	Elastic electron backscattering from silicon surfaces: effect of surface roughness. Surface and Interface Analysis, 2002, 34, 215-219.	1.8	15
89	On line shape analysis in X-ray photoelectron spectroscopy. Surface Science, 2001, 470, 325-336.	1.9	35
90	Escape probability of photoelectrons from silver sulphide. Surface Science, 2001, 473, 8-16.	1.9	27

#	Article	IF	CITATIONS
91	A theoretical investigation of photoemission spectra from (GaAs)2(AlAs)2 superlattices. Journal of Electron Spectroscopy and Related Phenomena, 2001, 114-116, 1127-1132.	1.7	1
92	Elastic electron backscattering from overlayer/substrate systems. Surface and Interface Analysis, 2001, 31, 825-834.	1.8	19
93	Valence-band photoemission fromGaAs(100)â^'c(4×4). Physical Review B, 2001, 63, .	3.2	14
94	One-step photoemission calculations for ideal GaAs(001) and AlAs(001) surfaces and(GaAs)m(AlAs)nsuperlattices. Physical Review B, 2001, 63, .	3.2	13
95	Inelastic mean free path measurements of electrons near nickel surfaces. Surface and Interface Analysis, 2000, 30, 217-221.	1.8	9
96	Measurements of the escape probability of photoelectrons and the inelastic mean free path in silver sulphide. Surface and Interface Analysis, 2000, 30, 222-227.	1.8	5
97	Determination of the electron inelastic mean free path in polyacetylene by elastic peak electron spectroscopy using different spectrometers. Applied Surface Science, 1999, 144-145, 168-172.	6.1	12
98	Determination of the inelastic mean free paths of electrons in copper and copper oxides by elastic peak electron spectroscopy (EPES). Surface and Interface Analysis, 1998, 26, 400-411.	1.8	27
99	Dependence of experimentally determined inelastic mean free paths of electrons on the measurement geometry. Surface Science, 1998, 412-413, 42-54.	1.9	55
100	Transfer of samples between separated ultrahigh vacuum instruments for semiconductor surface studies. Review of Scientific Instruments, 1998, 69, 2804-2805.	1.3	10
101	Measurement of the transmission function of the hemispherical energy analyser of ADES 400 electron spectrometer. European Physical Journal D, 1994, 44, 261-267.	0.4	78
102	Altered layer composition of sputtered InP(100) wafers: non-destructive concentration depth profiling. Surface Science, 1994, 318, 421-427.	1.9	14
103	Electronic and crystalline structure of Si/SiO2 interface modified by ArF excimer laser. Progress in Surface Science, 1990, 35, 197-199.	8.3	2
104	ArF excimer laser induced changes in the Si(100)/SiO2 interface studied in situ by ESCA and LEED. Applied Surface Science, 1989, 43, 297-300.	6.1	5